Curvature effects in carbon nanomaterials: Exohedral versus endohedral supercapacitors

Jingsong Huang,[a] Bobby G. Sumpter, and Vincent Meunier
Oak Ridge National Laboratory, Oak Ridge, Tennessee 37831-6367

Gleb Yushin
School of Materials Science and Engineering, Georgia Institute of Technology, Atlanta, Georgia 30332-0245

Cristelle Portet and Yury Gogotsi[b]
Department of Materials Science and Engineering, A.J. Drexel Nanotechnology Institute, Drexel University, Philadelphia, Pennsylvania 19104

(Received 15 January 2010; accepted 22 February 2010)

Capacitive energy storage mechanisms in nanoporous carbon supercapacitors hinge on endohedral interactions in carbon materials with macro-, meso-, and micropores that have negative surface curvature. In this article, we show that because of the positive curvature found in zero-dimensional carbon onions or one-dimensional carbon nanotube arrays, exohedral interactions cause the normalized capacitance to increase with decreasing particle size or tube diameter, in sharp contrast to the behavior of nanoporous carbon materials. This finding is in good agreement with the trend of recent experimental data. Our analysis suggests that electrical energy storage can be improved by exploiting the highly curved surfaces of carbon nanotube arrays with diameters on the order of 1 nm.

I. INTRODUCTION

New technologies for electrical energy conversion and storage are needed to harness sustainable and renewable energy sources, such as solar and wind power. Supercapacitors, or ultracapacitors, that store electrical energy in an electric double layer formed at the electrode/electrolyte interface have recently attracted a great deal of attention as efficient energy storage devices that feature high power density and exceptional cycle life.[1–7] As opposed to batteries, this energy storage mechanism does not involve chemical reactions, which are relatively slow. The performance of carbon-based supercapacitors has been significantly enhanced in the past decade, with the development of various nanoporous carbon materials with high surface areas, such as activated carbons, template carbons, and carbide-derived carbons, among others.[7–9] In order for supercapacitors to compete with existing battery technology, an energy density higher than currently available is essential while retaining a high power capability. Theoretical descriptions of charge storage processes at the electrode/electrolyte interface are needed to facilitate progress along this avenue.

Supercapacitors that use nanoporous carbons as electrode materials are commonly described as electric double-layer capacitors (EDLCs) because of the electric double layer formed at the electrode/electrolyte interface. In the field of supercapacitors, the formula of capacitance for nanoporous carbon materials is often borrowed from that of parallel-plate capacitors[10]:

$$C = \frac{\varepsilon_r \varepsilon_0 A}{d} \quad , \tag{1a}$$

$$\frac{C}{A} = \frac{\varepsilon_r \varepsilon_0}{d} \quad , \tag{1b}$$

where ε_r is the electrolyte dielectric constant, ε_0 is the permittivity of vacuum, A is the electrode specific surface area, and d is the effective thickness of the electric double layer. Equation (1) suggests that one way to improve the energy densities of EDLCs is to increase the surface area of porous carbon materials. It is often observed that higher capacitances are indeed obtained for carbons with higher surface area but the linear relationship between C and A generally cannot be established[11–13] and is a matter of debate. For supercapacitors with porous carbons as electrode materials that acquire their surface area primarily in the pores,

Address all correspondence to these authors.
[a]e-mail: huangj3@ornl.gov
[b]e-mail: gogotsi@drexel.edu
This author was an editor of this focus issue during the review and decision stage. For the *JMR* policy on review and publication of manuscripts authored by editors, please refer to http://www.mrs.org/jmr_policy
DOI: 10.1557/JMR.2010.0195

Eq. (1) may not be adequate to rationalize the electrochemical properties.

Recent experiments[14] and theoretical work[15] on nanoporous carbon materials with fine-tuned pore sizes have provided some critical information on the fundamental processes at the electrode/electrolyte interface, which is established inside the pores. It was found that for carbons with cylinder-shaped mesopores (diameter $>$ 2 nm), counterions in the electrolyte enter the pores and approach the pore walls to form an electric double-cylinder capacitor (EDCC).[15] This charge storage mechanism is of EDLC type, but the effect of pore curvature or pore size on capacitance in the mesopore regime is explicit, as follows[10]:

$$C = \frac{2\pi\varepsilon_r\varepsilon_0 L}{\ln(b/a)} \quad , \tag{2a}$$

$$\frac{C}{A} = \frac{\varepsilon_r\varepsilon_0}{b\,\ln[b/(b-d)]} \quad , \tag{2b}$$

where L is the pore length and a and b are the radii of the inner and outer cylinders, respectively. We found that Eq. (2) works well for carbon electrodes with cylinder-shaped mesopores because of the high concentration of electrolytes (typically $\geq$ 1 M) and the high conductivities of mesoporous carbons (typically $\geq$ 1 S cm^{-1}), both of which give rise to a small Debye screening length in the liquid and the solid.[16] Therefore, the electrode/electrolyte interface can be characterized by two compact layers of charges and a Helmholtz-like model is a rather good approximation. It is straightforward to reduce Eq. (2) for mesopores to Eq. (1) for the flat surface of macropores (diameter $>$ 50 nm) by using Taylor's expansion.[15] Turning back to the issue of the linear relationship between C and A, it is clear from Eq. (2) that only for carbons with the same (or approximately the same) pore size, C can be rigorously proportional to A. This requires that the analysis is conducted for carbons with finely-tuned pores or unimodal pore-size distribution,[17] which is hardly the case for most experiments where the $C-A$ relationship is discussed. However, this requirement for unimodal pore-size distribution does not speak against the desirability of hierarchical pore structures which contain macropores as ion-buffering reservoirs, mesopores facilitating ion transport, and micropores for optimal charge storage. For hierarchical pore structures, see Wang et al.[17]

For micropores (diameter $<$ 2 nm), the small pores do not allow the formation of an inner cylinder inside the pores. Unlike the double-layer charge storage mechanism in EDLC and EDCC, desolvated or partially desolvated counterions can enter micropores and line up along the pore axis to form an electric wire-in-cylinder capacitor (EWCC). In this regime, the capacitance of EWCCs remains pore size dependent as shown in the following equation[15]:

$$\frac{C}{A} = \frac{\varepsilon_r\varepsilon_0}{b\ln(b/a_0)} \quad , \tag{3}$$

where a_0 is the radius of the counterions. With Eq. (3), we were able to rationalize the anomalous increase in capacitance with decreasing pore size for carbide-derived carbons with a narrow distribution of sub-nanometer pores.[14] That analysis yielded an a_0 (2.30 Å) in good agreement with ion sizes and an ε_r (2.23) close to the vacuum value of 1, implying that the solvation shells of counterions are (at least partially) removed.[15]

The common feature of nanoporous carbon supercapacitors is that counterions enter pores to form endohedral supercapacitors, which have negative surface curvature. Graphene-based materials with zero curvature are also potential electrode materials with high surface areas and excellent conductivities.[18] While negative curvature for EDCC/EWCC and zero curvature for EDLC have been a recurrent subject of attention, much less emphasis has been given to positive curvature. Examples of positively curved surfaces are the external surfaces of nonporous zero-dimensional (0-D) carbon onions and one-dimensional (1-D) capped carbon nanotubes (CNTs) (Fig. 1). For these materials, counterions can only reside on the outer surfaces, leading to exohedral supercapacitors.[19] Recently, several experiments have been performed on carbon onions,[20–22] and vertically aligned CNT arrays,[23,24] providing results that show superior rate capabilities of exohedral supercapacitors. In particular, those electrodes can be charged at a high rate, approaching electrolytic capacitors. The objective of this work is to provide a theoretical analysis of exohedral supercapacitors and compare it with the available experimental data for carbon onions and carbon nanotubes. We expect that this analysis will facilitate the development of supercapacitors with improved energy storage capabilities.

II. THEORETICAL MODELS

As can be seen in Fig. 1, solvated counterions approach the surface of an electrically charged carbon onion particle, approximated as a solid sphere, to form an exohedral electric double-sphere capacitor (xEDSC). For CNTs, solvated counterions and the tube's outer wall form an exohedral electric double-cylinder capacitor (xEDCC). These two exohedral capacitors are represented schematically by their cross-section in Fig. 2, where the outer sphere/cylinder of radius b and the inner sphere/cylinder of radius a are separated by the effective double-layer thickness d. The capacitance of xEDSC is given as[10]:

$$C = \frac{4\pi\varepsilon_r\varepsilon_0\, ab}{b-a} \quad , \tag{4a}$$

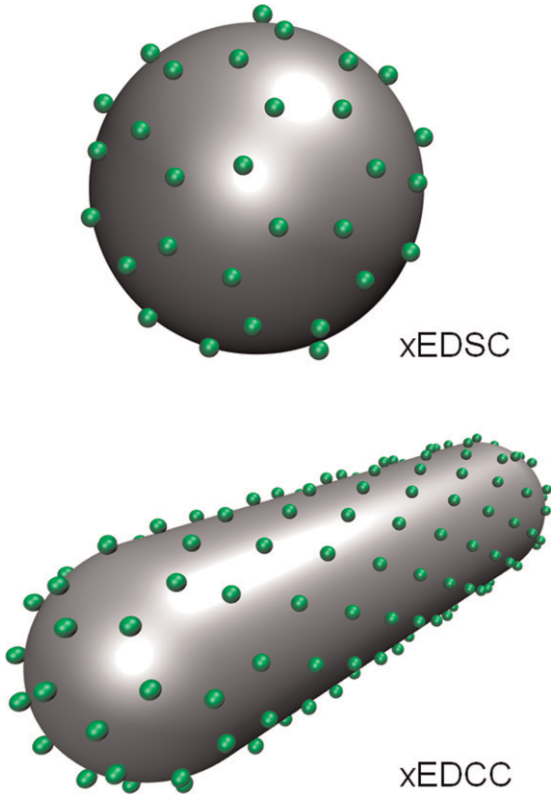

FIG. 1. Steric views of a charged zero-dimensional carbon onion sphere and a one-dimensional capped carbon nanotube with electrolyte counterions (solvent molecules not shown) approaching the outer surfaces to form an exohedral electric double-sphere capacitor (xEDSC) and an exohedral electric double-cylinder capacitor (xEDCC), respectively. (color online)

$$\frac{C}{A} = \frac{\varepsilon_r \varepsilon_0 (a+d)}{ad} \quad , \tag{4b}$$

and, following Eq. (2a) for EDCC, the capacitance of xEDCC is:

$$\frac{C}{A} = \frac{\varepsilon_r \varepsilon_0}{a \ln[(a+d)/a]} \quad . \tag{5}$$

The different trends of exohedral capacitors are compared with the endohedral counterparts as a function of particle diameter or pore size in Fig. 3. The horizontal line (EDLC) and curve a (EDCC) were calculated using Eqs. (1b) and (2b), respectively, with the parameters $\varepsilon_r = 9.63$ and $d = 8.86$ Å, while curve b (EWCC) was calculated using Eq. (3) with $\varepsilon_r = 2.23$ and $a_0 = 2.30$ Å. These parameters were obtained previously by fitting experimental data.[15] A notable feature of curve a is that there exists a trend of slightly increasing normalized capacitance with increasing pore size in zone II and it approaches asymptotically the EDLC line in zone III. For macropores (diameters > 50 nm), the EDCC is virtually equivalent to EDLC. This shows that the pore curvature/size effect is negligible for macropores, while it is significant for small-diameter pores. Meanwhile, curve b exhibits an anomalous increase in capacitance in the subnanometer pore regime.

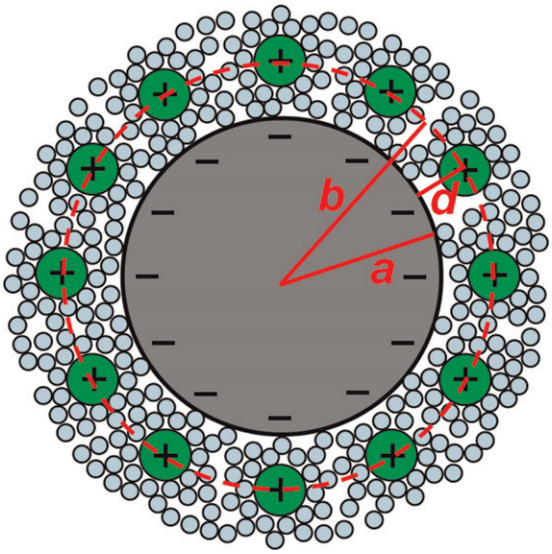

FIG. 2. Cross-section of an exohedral capacitor, consisting of two layers of charges with radii a and b for the inner and outer spheres/cylinders, respectively, separated by the effective double-layer thickness d. (color online)

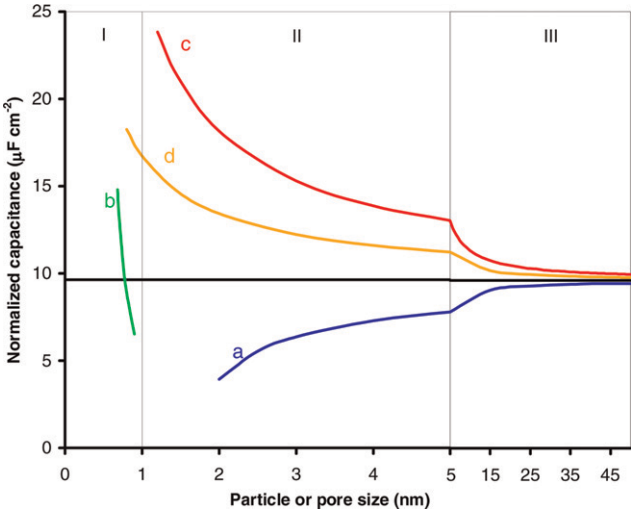

FIG. 3. Normalized capacitances as a function of particle/pore size for endohedral capacitors (curves a and b for mesoporous and microporous carbons, respectively) and exohedral capacitors (curves c and d for zero-dimensional spheres and one-dimensional tubes, respectively). When the particle or pore size is large, all curves approach asymptotically the horizontal line representing a parallel-plate capacitor. (color online)

Following Eqs. (4b) and (5), we calculated the capacitance of xEDSC and xEDCC by using the same set of parameters as for curve a, assuming that these parameters are approximately independent of surface curvature (comparable values are indeed obtained by fitting experimental data; see results below). As can be seen in Fig. 3,

the normalized capacitances of spheres and tubes are above the horizontal line of EDLC and both increase with decreasing tube diameter and particle size. This is in sharp contrast to the results of curves a and b, especially in that these exohedral capacitors retain the trend of increasing capacitance with decreasing particle size even in the ~1 nm particle size range. In addition, the capacitance of spheres (curve c) increases faster than that of tubes (curve d), because a sphere has locally two positive principal Gaussian curvatures while a tube only has one (the other being zero, along the axis). The extrapolation of curves c and d from zone II into zone III both approach asymptotically the EDLC line.

III. RESULTS AND DISCUSSION

With the different patterns established in Fig. 3, we now examine published experimental results for 0-D onions and 1-D CNTs to test the theoretical model for exohedral supercapacitors described above.

Recent electrochemical studies on the capacitance of 0-D carbon onions with an organic electrolyte of 1.5 M tetraethylammonium tetrafluoroborate in acetonitrile[20] display a trend similar to that of xEDSC as shown by curve c in Fig. 3. As can be seen in Fig. 4, the highest normalized capacitance value is for nanodiamond soot (diamond nanocrystals coated with fullerene-like carbon shells). The capacitance values of carbon onions decrease with increasing average particle size, which is correlated with increasing annealing temperature from 1200, 1500, 1800, to 2000 °C. Particle size in Fig. 4 was estimated from high resolution transmission electron microscopy to increase from an average of ~5 nm for nanodiamond soot to 5.5–7.0 nm for carbon onions upon annealing. High-temperature annealing converts the sp^3 carbon of nanodiamonds into the sp^2 carbon in the concentric fullerene-like layers of carbon onions, increasing the particle size due to decreasing density (2.27 g/cm^3 in graphite compared to 3.51 g/cm^3 in diamond). The number of fullerene-like layers grows with increasing annealing temperature as a higher degree of graphitization is achieved.[21,25] Polygonization of nanoparticles occurs after heating to 2000 °C. Such a high temperature also leads to the slow decrease in the specific surface area,[20] because of sintering (agglomeration) of the smallest particles. Formation of perfectly ordered carbon shells and healing of defects in the sp^2 shell wall may also contribute to the decrease of SSA with temperature. All of these changes including particle size, polygonization, and agglomeration contribute to the decrease in surface curvature.

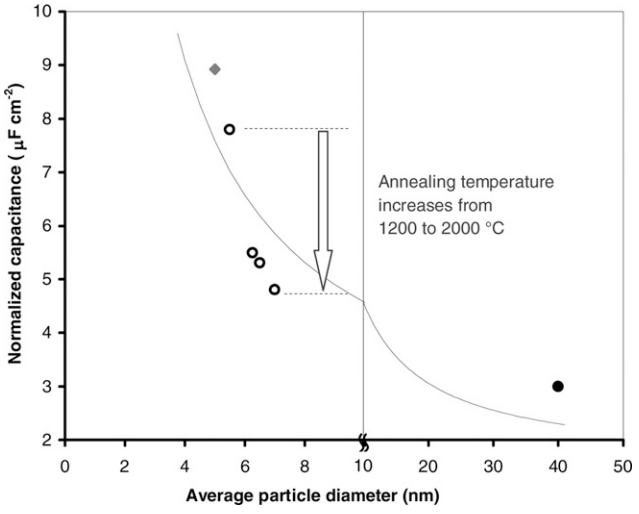

FIG. 4. Normalized capacitances of nanodiamond soot (♦), carbon onions (○), and carbon black (●) as a function of average particle diameter (annealing temperature shown by the arrow) with an organic electrolyte of 1.5 M tetraethylammonium tetrafluoroborate in acetonitrile.[20] The fitting curve was obtained with Eq. (4b), showing a trend that capacitance increases with decreasing particle diameter.

In Fig. 4, we supplement the data set of carbon onions with the results for a carbon black sample that has primarily outer surfaces exposed to an electrolyte and does not have subnanometer pores on each particle.[20] This carbon black has a particle size of approximately 40 nm, and a gravimetric capacitance of 1.5 F/g. The previously reported capacitance[20] of 2 F/g is corrected to 1.5 F/g with the background capacitance coming from the polyurethane-based conductive paint included, which is negligible for porous carbon or carbon onion electrodes. As a result, the normalized capacitance is 3 μF/cm^2. This value corroborates the trend shown in Fig. 4 and also appears to be an asymptotic limit of the carbon onion data. Compared to the larger-pore capacitance about 10 μF/cm^2 for the endohedral capacitors (Fig. 3), the normalized capacitance values in Fig. 4 are rather low, as a result of particle agglomeration during electrode preparation process which reduces the particle surface areas measured for the powder samples (see discussion below).

This trend is however absent for the carbon onions annealed at 897 and 1147 °C reported by Bushueva et al.[21] The nanodiamonds used for making carbon onions were subjected to acid treatment to remove carbons other than sp^3 structures.[25] Consequently, the conductivities of carbon onions annealed at 897 and 1147 °C are up to seven orders of magnitude lower than those of carbon onions annealed above 1327 °C and the capacitances are adversely affected by the low conductivities. In contrast, all the carbon onions reported by Portet et al.[20] have comparable conductivities on the order of 1 S cm^{-1} and only the nanodiamond soot has a conductivity of about two orders of magnitude lower, which may be responsible for its lower gravimetric capacitance than carbon onions.[20] The nanodiamond soot reported by Portet et al.[20] is still conductive because of the sp^2 structures in the amorphous carbon, fullerene-like shells, and graphitic ribbons.[26]

In addition to particle size and conductivities, defects and micropores also affect capacitance. Defects in

nanodiamond soot and carbon onions at lower annealing temperature allow local field concentrations (sharp edges or points dramatically increase the electric-field strength at those edges or points) and/or distortion of the solvation shell near the defect. These defect-driven effects might contribute to localized retention of ions and therefore higher capacitances.[20] Micropores may strip off the solvation shells of electrolyte ions leading to closer attraction of an ion center to the carbon surface, thereby increasing the normalized capacitance. Annealing at high temperature seals the micropores, and thus decreases the capacitance. However, this effect may be small due to the negligible amount of micropores in the nanodiamond soot and carbon onions, as confirmed by our CO_2 and Ar adsorption experiments (not shown).

In spite of these different effects on capacitance, we find it helpful for discussion to present the fitting results for the experimental data in Fig. 4 using Eq. (4b). The electrochemical parameters obtained are: $\varepsilon_r = 17.03$ (4.80), $d = 9.73$ (10.91) nm, and $R^2 = 0.759$, where the numbers in the parentheses are standard errors. The ε_r value of 17.03 is much smaller than the bulk value of acetonitrile ($\varepsilon_r = 36$) and is close to that of mesoporous carbons obtained from an earlier fit with Eq. (2b).[15,19] The effective double-layer thickness d seems to be too large compared to the dimension of the ions,[15,19] which is usually approximated as the double layer thickness. However, in light of the large standard error, an accurate d value was not obtained. The fitting quality is not as good as for the mesoporous carbons, as reflected from the large standard errors and the relatively low R^2 value. Unlike endohedral supercapacitors,[15,19] it is more challenging to fit the data perfectly. The reason is essentially twofold. First, nanodiamond soot and carbon onions are not mono-dispersed and do not have a narrow particle size distribution.[20] Second, isolated carbon onions are connected to each other, making them conductive, and therefore the model of xEDSC for isolated spheres is not completely realistic. As can be seen in Fig. 5, particle agglomeration also induces negative curvature at the contact points. In addition, the pseudopores between particles also have negative curvature. The presence of negatively curved areas cancels out the beneficial effects of positively curved carbon onions. We stress that, in spite of the low fitting quality, the distinct behavior of an exohedral supercapacitor is captured for carbon onions, as indicated by the trend, which is opposite to that of endohedral supercapacitors.

Due to the complex effects of particle size, conductivities, defects, micropores, and close contacts between particles on normalized capacitance for 0-D carbon onions, it is desirable to examine 1-D CNTs with different tube diameters, where the various effects of conductivities, defects, micropores, and close contacts may become less profound. Recent experimental results of

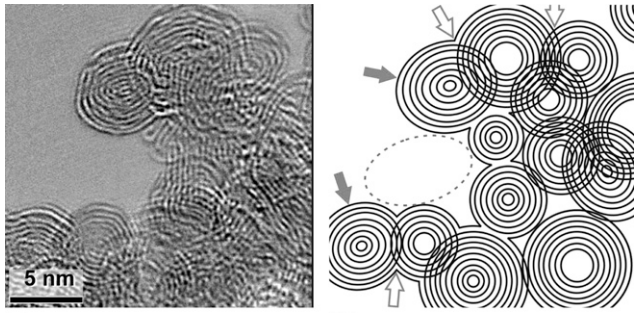

FIG. 5. (a) Transmission electron microscopy (TEM) micrograph and (b) the schematic diagram of carbon onions agglomerating together with positive and negative curvatures as indicated by the solid and hollow arrows, respectively, and with pseudopores as indicated by the dashed circle. TEM observations of carbon nanoparticles have been performed using a JEOL 2010F microscope operated at an acceleration voltage of 200 kV. TEM samples were prepared by a one-minute sonication of the powders in ethanol and deposition on a lacey-carbon coated copper grid (200 mesh).

1-D CNTs with an organic electrolyte of 1.96 M triethylmethylammonium tetrafluoroborate in propylene carbonate also exhibit a trend similar to that of the 0-D carbon onions, which further supports the effects of positive surface curvature identified herein. Ishikawa and coworkers prepared vertically aligned multiwalled CNTs (MWCNTs) on an Al current collector and studied the electrochemical properties of these MWCNT-based capacitors.[23] A thin layer of conductive cement between the aligned MWCNT arrays and the electrode substrate offers a strong mechanical adhesion and low contact resistances between CNTs and the current collector, which are essential to study the intrinsic capacitance performance of CNTs that is difficult to be probed by using entangled (disordered) CNTs. The size of the MWCNTs ranges from 14 to 37 nm in diameter. The tubes do not undergo agglomeration that is observed for carbon onions. The inter-tube voids are on the order of tens of nanometers and therefore there are no pseudopores in these CNT arrays. It was found that the gravimetric capacitance increases with decreasing average tube diameter (Fig. 6), showing the trend for an xEDCC depicted by curve d in Fig. 3. The gravimetric capacitance in Fig. 6 is rather low compared to that of nanoporous carbon supercapacitors which is usually on the order of 100 F/g in organic electrolytes. This should be ascribed to the extra mass coming from the inner CNT walls, which do not directly contribute to energy storage. The gravimetric capacitance of double-walled CNT arrays is greatly enhanced as compared to MWCNT arrays.[24] Even higher gravimetric capacitance can be expected for single-walled CNT arrays, although this is actually not observed experimentally,[27] simply because not all single-walled CNTs in the array exhibit metallic conductivity, which is desirable to keep the series resistance low. Due to the lack of

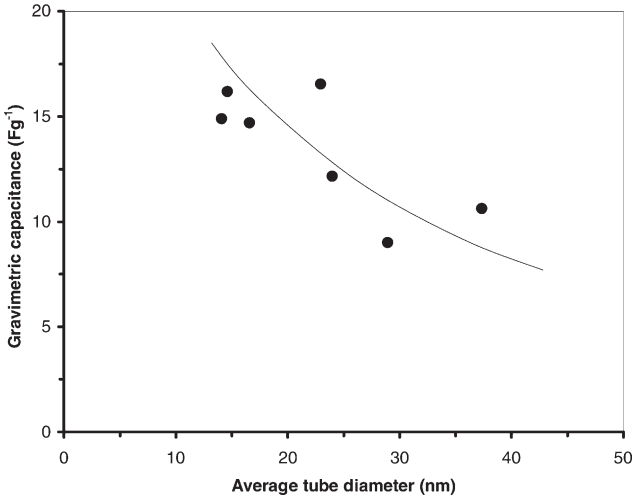

FIG. 6. Gravimetric capacitances of vertically aligned MWCNTs with an organic electrolyte of 1.96 M triethylmethylammonium tetrafluoroborate in propylene carbonate as a functional of average tube diameters.[23] The curve is provided to guide the eye, showing a trend that capacitance increases with decreasing tube diameter.

specific surface area data in the work of Honda et al.,[23] we are unable to convert the gravimetric capacitance to normalized capacitance or to fit the data by Eq. (5). Assuming small changes of specific surface area among the MWCNT arrays with different diameters in the Ishikawa experiment, one may retain the trend of increasing normalized capacitance with decreasing tube diameter, albeit the changes may be less pronounced as can be expected from the calculations shown in zone III of Fig. 3.

It is worth pointing out that the variation in CNT lengths may work against the trend shown in Fig. 6 as the lengths of CNT arrays decrease with increasing tube diameters.[23] In a different experiment comparing shorter CNTs that have lengths <1 μm and diameters in the 10–20 nm range with longer CNTs that have lengths >100 μm and diameters in the 10–40 nm range, Ishikawa and co-workers found that shorter CNTs have higher normalized capacitance (20.6 μF/cm^2) than longer CNTs (14.5 μF/cm^2). They ascribed this difference to the number of edges per unit weight.[28] Similar to the higher capacitance of graphene edges than that of its basal planes,[8] the capacitance of CNT edges is expected to be higher than that of the CNT sidewalls. We note that such CNT edge effects in fact may originate from the end caps of CNTs since most tubes should be capped. The end caps are hemispheres and have higher curvature than sidewalls. Therefore, in the context of surface curvature, the disparity in normalized capacitance reported by Honda et al.[28] can be rationalized by both the smaller tube diameters and the higher number of end caps per unit tube length for the shorter tubes. Zhang et al. prepared aligned MWCNT array with CNTs of 14 nm in diameter on Ni foil and found that the normalized capacitance is 33.7 μF/cm^2 in an organic electrolyte of 1 M tetraethylammonium hexafluorophosphate.[29] These normalized capacitance values are high for CNTs with diameters on the order of tens of nm but they follow the trend we discussed above.

Compared to endohedral supercapacitors in which electrolyte ions have to diffuse deep inside the pores or undergo a desolvation process before entering micropores, for exohedral supercapacitors that are based on 0-D carbon onions or 1-D CNT arrays, electrolyte ions have relatively easy access to the carbon/electrolyte interface. The mass transport and desolvation reaction kinetics associated with nanoporous carbons may increase the equivalent series resistance for endohedral supercapacitors. Therefore, exohedral supercapacitors have rapid charge/discharge rates owing to the absence of deep pores, as demonstrated by the high cyclic voltammetry scanning rate of 9 V/s for carbon onions as compared to the scanning rate of 1 V/s for microporous carbide-derived carbons, at which the electrodes can still maintain capacitive behavior using the cavity microelectrode technique.[30] One order of magnitude higher rates have been measured in our recent experiments (unpublished). Extraordinary rate capabilities were also observed for vertically aligned MWCNT arrays on an Al substrate where no deviation from double-layer capacitance behavior was observed at a high galvanostatic discharge current density of 10 A/g or at an extremely high cyclic voltammetry scanning rate of 50 V/s.[23] These rapid electrochemical responses make exohedral supercapacitors suitable for high-power applications.[20] Our theoretical analysis shows that the decrease in the particle diameter can lead to increased energy storage capacity due to both increasing SSA and increasing capacitance per unit of surface area.

IV. CONCLUSIONS

In summary, we have shown that, for exohedral supercapacitors that use 0-D carbon onions and 1-D CNT arrays as electrode materials, the positive curvature causes normalized capacitance increases with decreasing particle size or tube diameter. While a reliable fitting of experimental data is hampered by the complex effects of conductivities, defects, micropores, and close contacts between particles on normalized capacitance for 0-D carbon onions, a systematic study is possible by using aligned CNTs directly grown or pasted on conducting substrates. Nevertheless, we have found a trend that is characteristic of exohedral materials and is in sharp contrast to the behavior of nanoporous carbon materials. This trend may also be found in other exohedral carbon materials such as nonporous carbon nanofibers[31] or in various silica-templated carbons that have a combination of endohedral pores within the carbon nanorods and exohedral pores between the nanorods.[32] This finding offers an opportunity to enhance the performance of

carbon-based supercapacitors. For these exohedral supercapacitors, the smallest conductive carbon onions and CNTs should be exploited. The argument presented for exohedral supercapacitors is based on capacitance normalized with specific surface area and a high normalized capacitance does not necessarily correlate with exceptional gravimetric or volumetric capacitance, especially in light of the moderate specific surface areas of carbon onions and CNTs. Nevertheless, it is important to keep this trend in mind while optimizing the surface area and density of these exohedral carbon materials.

ACKNOWLEDGMENTS

We gratefully acknowledge the support from the Laboratory Directed Research and Development Program of Oak Ridge National Laboratory (ORNL) and from the Center for Nanophase Materials Sciences, sponsored by the Division of Scientific User Facilities, U.S. Department of Energy. G. Yushin was supported by the Air Force Office of Scientific Research, Physics and Electronics Directorate. Y. Gogotsi was supported as part of the Fluid Interface Reactions, Structures and Transport (FIRST) Center, an Energy Frontier Research Center funded by the U.S. Department of Energy, Office of Science, Office of Basic Energy Sciences under Award No. ERKCC61.

REFERENCES

1. B.E. Conway: *Electrochemical Supercapacitors: Scientific Fundamentals and Technological Applications* (Kluwer Academic/Plenum, New York, 1999).
2. U.S. Department of Energy: Basic research needs for electrical energy storage: Report of the basic energy sciences workshop on electrical energy storage (http://www.sc.doe.gov/bes/reports/files/EES_rpt.pdf), 2007.
3. The special issue on electrochemical capacitors. *Electrochem. Soc. Interface* **17,** 31 (2008).
4. J.R. Miller and P. Simon: Materials science—Electrochemical capacitors for energy management. *Science* **321,** 651 (2008).
5. A. Burke: Ultracapacitors: Why, how, and where is the technology. *J. Power Sources* **91,** 37 (2000).
6. R. Kötz and M. Carlen: Principles and applications of electrochemical capacitors. *Electrochim. Acta* **45,** 2483 (2000).
7. P. Simon and Y. Gogotsi: Materials for electrochemical capacitors. *Nat. Mater.* **7,** 845 (2008).
8. A.G. Pandolfo and A.F. Hollenkamp: Carbon properties and their role in supercapacitors. *J. Power Sources* **157,** 11 (2006).
9. E. Frackowiak: Carbon materials for supercapacitor application. *Phys. Chem. Chem. Phys.* **9,** 1774 (2007).
10. P.A. Tipler: *Physics* (Worth, New York, 1976), pp. 768–771.
11. H. Shi: Activated carbons and double layer capacitance. *Electrochim. Acta* **41,** 1633 (1996).
12. C. Vix-Guterl, E. Frackowiak, K. Jurewicz, M. Friebe, J. Parmentier, and F. Béguin: Electrochemical energy storage in ordered porous carbon materials. *Carbon* **43,** 1293 (2005).
13. M. Sevilla, S. Alvarez, T.A. Centeno, A.B. Fuertes, and F. Stoeckli: Performance of templated mesoporous carbons in supercapacitors. *Electrochim. Acta* **52,** 3207 (2007).
14. J. Chmiola, G. Yushin, Y. Gogotsi, C. Portet, P. Simon, and P.L. Taberna: Anomalous increase in carbon capacitance at pore size less than 1 nanometer. *Science* **313,** 1760 (2006).
15. J. Huang, B.G. Sumpter, and V. Meunier: Theoretical model for nanoporous carbon supercapacitors. *Angew. Chem. Int. Ed.* **47,** 520 (2008).
16. H. Gerischer: The impact of semiconductors on the concepts of electrochemistry. *Electrochim. Acta* **35,** 1677 (1990).
17. D.W. Wang, F. Li, M. Liu, G.Q. Lu, and H.M. Cheng: 3D aperiodic hierarchical porous graphitic carbon material for high-rate electrochemical capacitive energy storage. *Angew. Chem. Int. Ed.* **47,** 373 (2008).
18. M.D. Stoller, S.J. Park, Y.W. Zhu, J.H. An, and R.S. Ruoff: Graphene-based ultracapacitors. *Nano Lett.* **8,** 3498 (2008).
19. J. Huang, B.G. Sumpter, and V. Meunier: A universal model for nanoporous carbon supercapacitors applicable to diverse pore regimes, carbon materials, and electrolytes. *Chem. Eur. J.* **14,** 6614 (2008).
20. C. Portet, G. Yushin, and Y. Gogotsi: Electrochemical performance of carbon onions, nanodiamonds, carbon black and multiwalled nanotubes in electrical double layer capacitors. *Carbon* **45,** 2511 (2007).
21. E.G. Bushueva, P.S. Galkin, A.V. Okotrub, L.G. Bulusheva, N.N. Gavrilov, V.L. Kuznetsov, and S.I. Moiseekov: Double layer supercapacitor properties of onion-like carbon materials. *Phys. Status Solidi B* **245,** 2296 (2008).
22. K. Lian, S. Park, and Y. Gogotsi: Pseudocapacitive behavior of carbon nanoparticles modified by phosphomolybdic acid. *J. Electrochem. Soc.* **156,** A921 (2009).
23. Y. Honda, T. Haramoto, M. Takeshige, H. Shiozaki, T. Kitamura, K. Yoshikawa, and M. Ishikawa: Performance of electric double-layer capacitor with vertically aligned MWCNT sheet electrodes prepared by transfer methodology. *J. Electrochem. Soc.* **155,** A930 (2008).
24. Y. Honda, M. Takeshige, H. Shiozaki, T. Kitamura, K. Yoshikawa, S. Chakrabarti, O. Suekane, L.J. Pan, Y. Nakayama, M. Yamagata, and M. Ishikawa: Vertically aligned double-walled carbon nanotube electrode prepared by transfer methodology for electric double layer capacitor. *J. Power Sources* **185,** 1580 (2008).
25. V.L. Kuznetsov, Y.V. Butenko, A.L. Chuvilin, A.I. Romanenko, and A.V. Okotrub: Electrical resistivity of graphitized ultra-disperse diamond and onion-like carbon. *Chem. Phys. Lett.* **336,** 397 (2001).
26. S. Osswald, G. Yushin, V. Mochalin, S.O. Kucheyev, and Y. Gogotsi: Control of sp^2/sp^3 carbon ratio and surface chemistry of nanodiamond powders by selective oxidation in air. *J. Am. Chem. Soc.* **128,** 11635 (2006).
27. T. Iwasaki, T. Maki, D. Yokoyama, H. Kumagai, Y. Hashimoto, T. Asari, and H. Kawarada: Highly selective growth of vertically aligned double-walled carbon nanotubes by a controlled heating method and their electric double-layer capacitor properties. *Phys. Status Solidi RRL* **2,** 53 (2008).
28. Y. Honda, T. Ono, M. Takeshige, N. Morihara, H. Shiozaki, T. Kitamura, K. Yoshikawa, M. Morita, M. Yamagata, and M. Ishikawa: Effect of MWCNT bundle structure on electric double-layer capacitor performance. *Electrochem. Solid-State Lett.* **12,** A45 (2009).
29. H. Zhang, G.P. Cao, and Y.S. Yang: Electrochemical properties of ultra-long, aligned, carbon nanotube array electrode in organic electrolyte. *J. Power Sources* **172,** 476 (2007).
30. C. Portet, J. Chmiola, Y. Gogotsi, S. Park, and K. Lian: Electrochemical characterizations of carbon nanomaterials by the cavity microelectrode technique. *Electrochim. Acta* **53,** 7675 (2008).
31. D. Hulicova-Jurcakova, X. Li, Z.H. Zhu, R. de Marco, and G.Q. Lu: Graphitic carbon nanofibers synthesized by the chemical vapor deposition (CVD) method and their electrochemical performances in supercapacitors. *Energy Fuels* **22,** 4139 (2008).
32. Y. Korenblit, M. Rose, E. Kockrick, L. Borchardt, A. Kvit, S. Kaskel, and G. Yushin: High-rate electrochemical capacitors based on ordered mesoporous silicon carbide-derived carbon. *ACS Nano* **4,** 1337 (2010).